

The background of the slide is a photograph of a cityscape, likely Boulder, Colorado, featuring a mix of modern and traditional buildings, green spaces, and a range of snow-capped mountains in the distance under a clear blue sky. The image is partially obscured by large, dark blue geometric shapes that frame the text on the left side.

XCIMER

MFEM Workshop 2024

Towards Predictive Modeling of the World's Most Powerful Fusion Laser at Xcimer

Milan Holec

10/23/2024

This is laser fusion on the grid

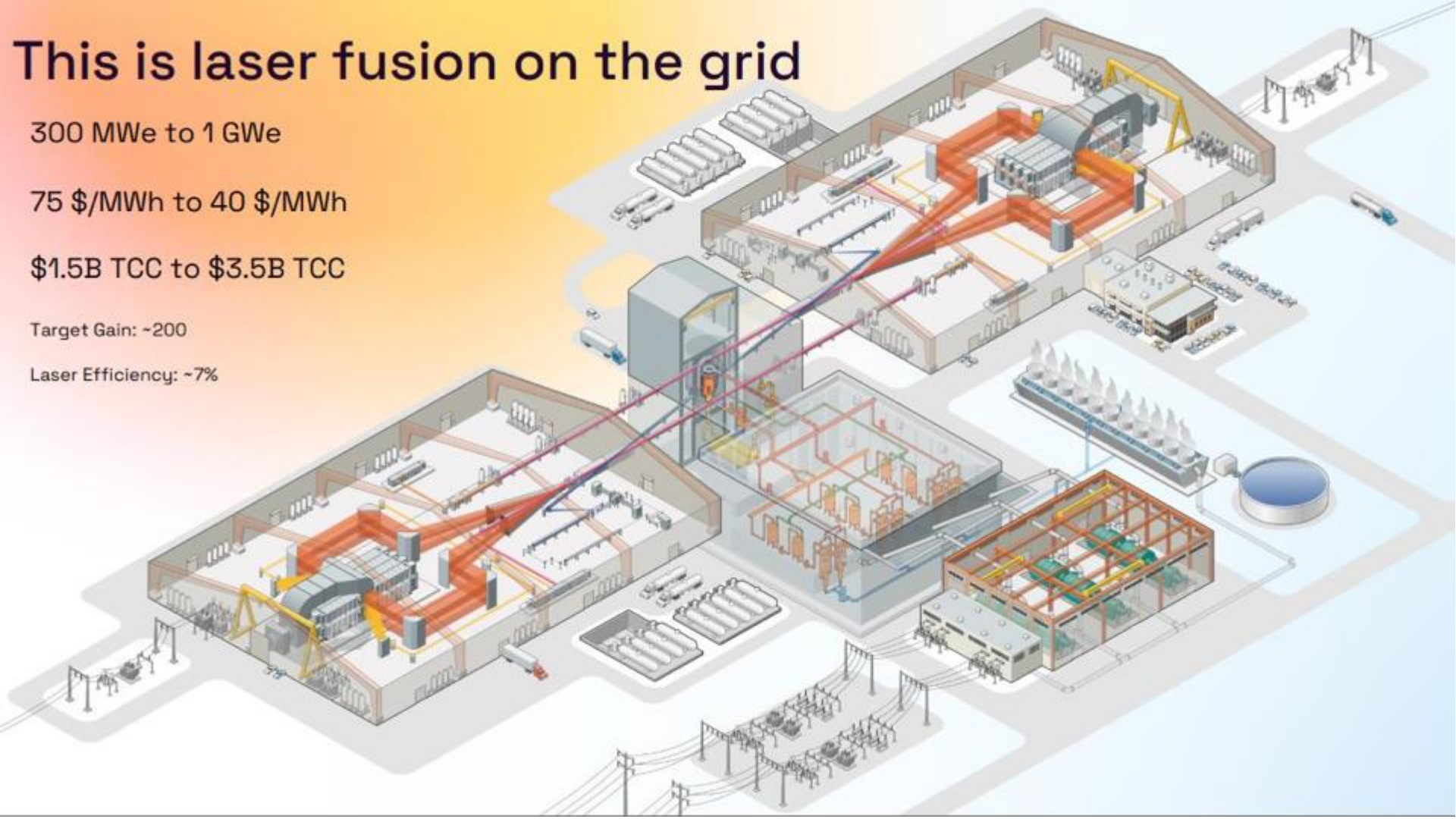
300 MWe to 1 GWe

75 \$/MWh to 40 \$/MWh

\$1.5B TCC to \$3.5B TCC

Target Gain: ~200

Laser Efficiency: ~7%



Team

Computing & Theory

- nonlinear optics
- plasma kinetics
- radhydro/MHD
- applied math
- HPC
- data science



Milan Holec



Daniel Treiman



David Schmidt



Jacob Milberger



Rahul Kumar



Warren Colomb



Ernesto Barraza-Valdez

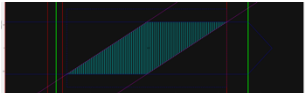
IRIS

digital twin / virtual beamline

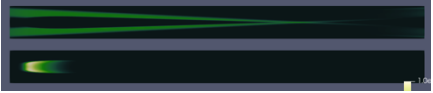


Iris (greek goddess of the rainbow and the messenger of the Olympian gods) is Xcimer's simulation code to predict the seed profile throughout the Phoenix system.

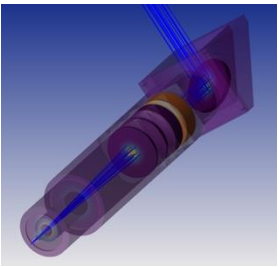
Fourier propagation (FFT)



Coupled-wave-system SBS (FEM)



Zemax



XEC



Modular system (model plugins)

Python, C++, Matlab
 Libraries: cws, ioglue, physutils, jeff, excalibur
 High-performance computing (HPC)
 MFEM-based high-order accuracy

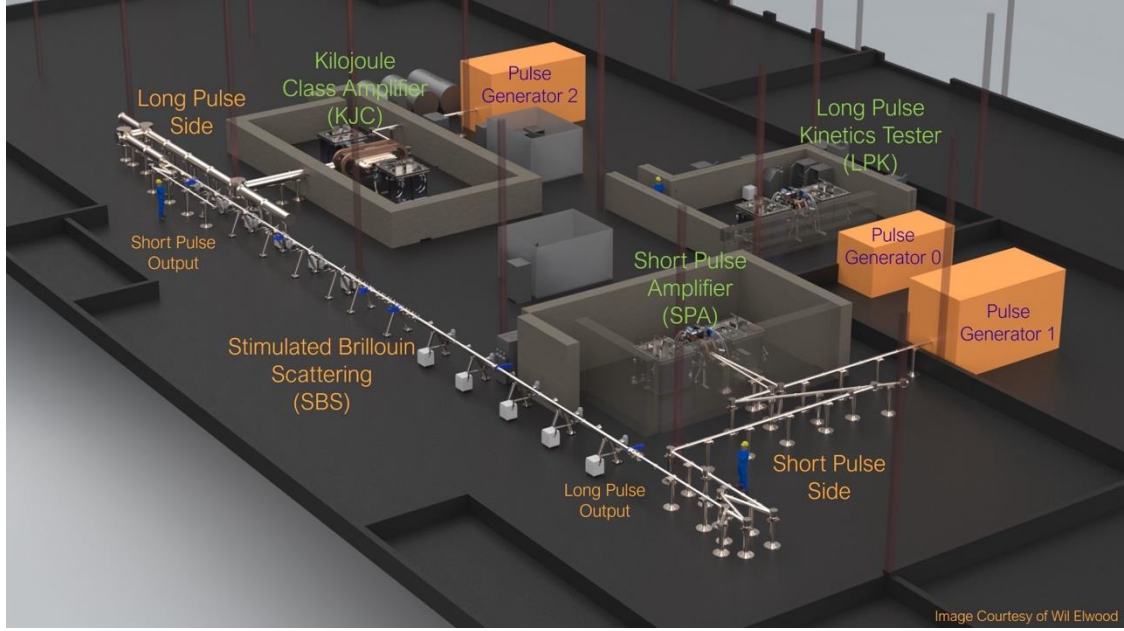
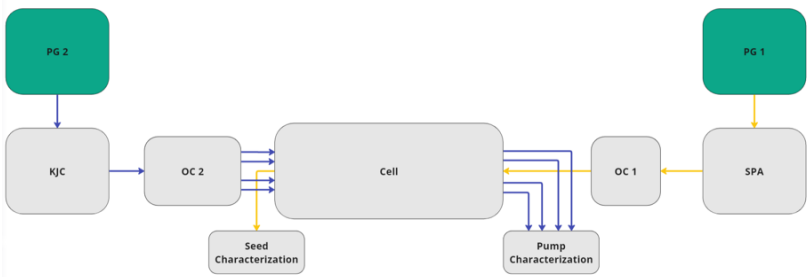


Image Courtesy of Wil Elwood



Gas SBS model

$$\nabla^2 \tilde{E} - \frac{n^2}{c^2} (\partial_{tt}^2 \tilde{E} - \alpha_E \partial_t \nabla^2 \tilde{E}) = \frac{\gamma_e}{4\pi\rho_0} \partial_{tt}^2 (\tilde{\rho} \tilde{E}),$$

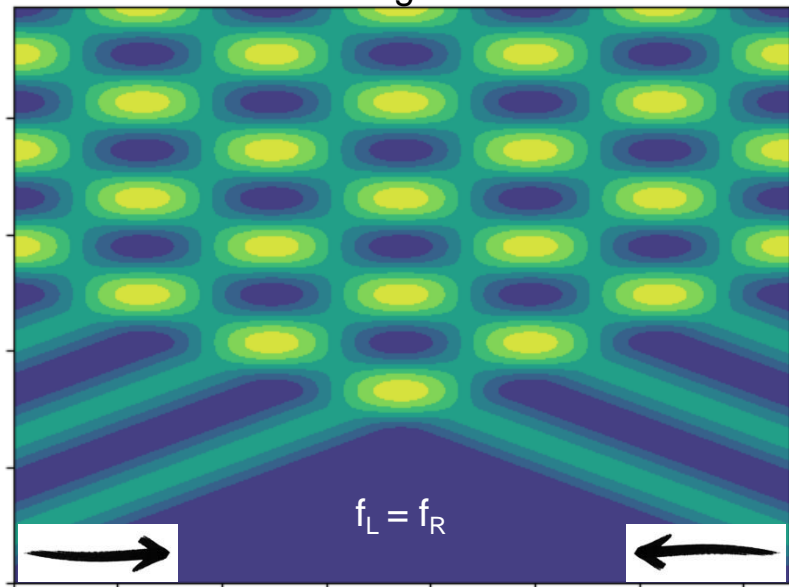
$$\nabla^2 \tilde{\rho} - \frac{\gamma}{v_s^2} (\partial_{tt}^2 \tilde{\rho} - \Gamma \partial_t \nabla^2 \tilde{\rho}) = \frac{\gamma \gamma_e}{v_s^2 8\pi} \nabla^2 \langle \tilde{E}^2 \rangle,$$

- Nonlinear Maxwell equations
- Wave optics: diffraction, self-focusing, speckles, ...
- **Three-wave** nonlinear optics (electrostriction)
- 248 nm wavelength vs 100 m beamline (10^9 dofs in 1D)
- High-frequency separation

```
[6]: # SIMULATION
      # Load hpc-cws-3d library
      import IRIS
      import cws
      # Assign desired boundary conditions
      config['pulseL_inflow'] = inflow_left_wave
      config['pulseR_inflow'] = inflow_right_wave
      config['cfl'] = 0.5
      # Run the simulation
      result = cws.beam1d(**config)
```

dt = 1.55e-18, hx = 9.3e-08
 Number of pulseR unknowns: 800
 Number of pulseL unknowns: 800
 Simulation of 3200 timesteps until 4.96e-15

Standing wave

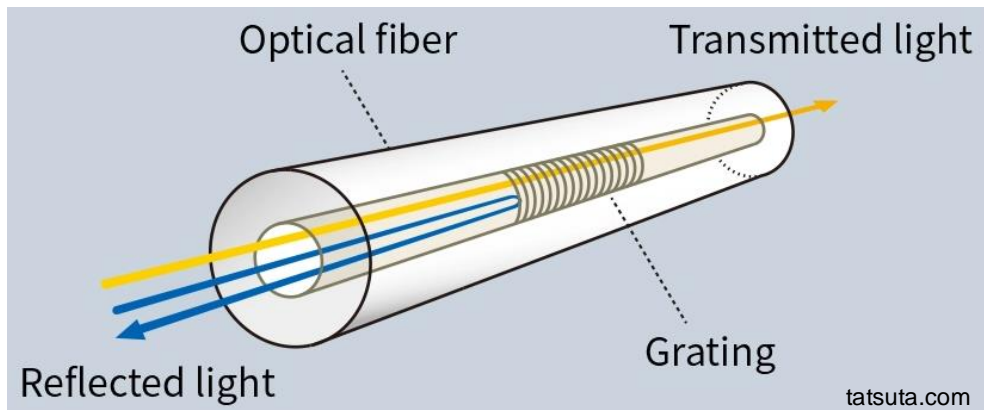


Base model

$$\partial_t A_0 + \frac{c \hat{\mathbf{k}}_0}{n} \cdot \nabla A_0 - \frac{ic}{2nk_0} \nabla^2 A_0 = -R |A_s|^2 A_0,$$

$$\partial_t A_s + \frac{c \hat{\mathbf{k}}_s}{n} \cdot \nabla A_s - \frac{ic}{2nk_s} \nabla^2 A_s = R^* |A_0|^2 A_s,$$

XEC



Gas SBS model

$$\nabla^2 \tilde{E} - \frac{n^2}{c^2} (\partial_{tt}^2 \tilde{E} - \alpha_E \partial_t \nabla^2 \tilde{E}) = \frac{\gamma_e}{4\pi\rho_0} \partial_{tt}^2 (\tilde{\rho} \tilde{E}),$$

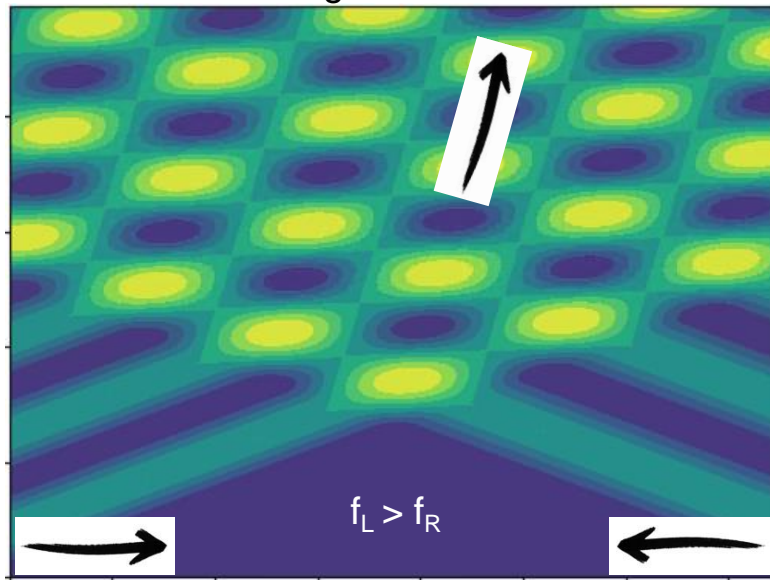
$$\nabla^2 \tilde{\rho} - \frac{\gamma}{v_s^2} (\partial_{tt}^2 \tilde{\rho} - \Gamma \partial_t \nabla^2 \tilde{\rho}) = \frac{\gamma \gamma_e}{v_s^2 8\pi} \nabla^2 \langle \tilde{E}^2 \rangle,$$

- Nonlinear Maxwell equations
- Wave optics: diffraction, self-focusing, speckles, ...
- **Three-wave** nonlinear optics (electrostriction)
- 248 nm wavelength vs 100 m beamline (10^9 dofs in 1D)
- High-frequency separation

```
[6]: # SIMULATION
      # Load hpc-cws-3d library
      IRIS
      import cws
      # Assign desired boundary conditions
      config['pulseL_inflow'] = inflow_left_wave
      config['pulseR_inflow'] = inflow_right_wave
      config['cfl'] = 0.5
      # Run the simulation
      result = cws.beam1d(**config)
```

dt = 1.55e-18, hx = 9.3e-08
 Number of pulseR unknowns: 800
 Number of pulseL unknowns: 800
 Simulation of 3200 timesteps until 4.96e-15

Moving acoustic wave

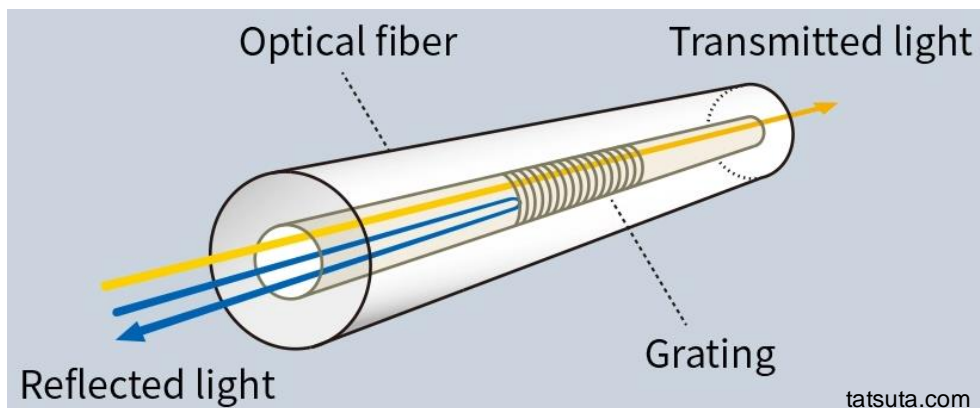


Base model

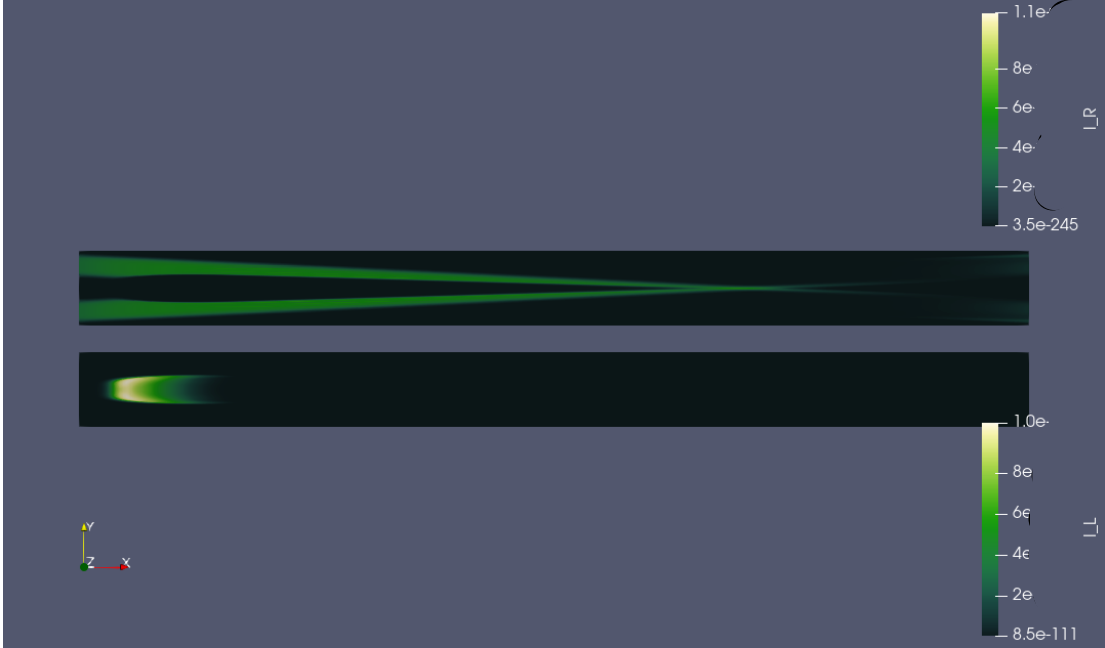
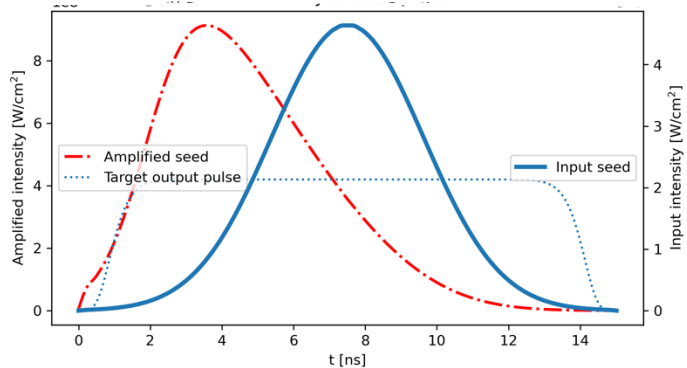
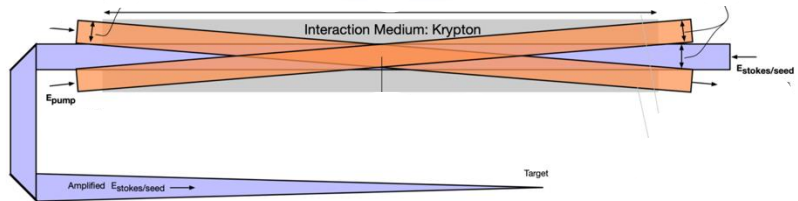
$$\partial_t A_0 + \frac{c \hat{\mathbf{k}}_0}{n} \cdot \nabla A_0 - \frac{ic}{2nk_0} \nabla^2 A_0 = -R |A_s|^2 A_0,$$

$$\partial_t A_s + \frac{c \hat{\mathbf{k}}_s}{n} \cdot \nabla A_s - \frac{ic}{2nk_s} \nabla^2 A_s = R^* |A_0|^2 A_s,$$

XEC



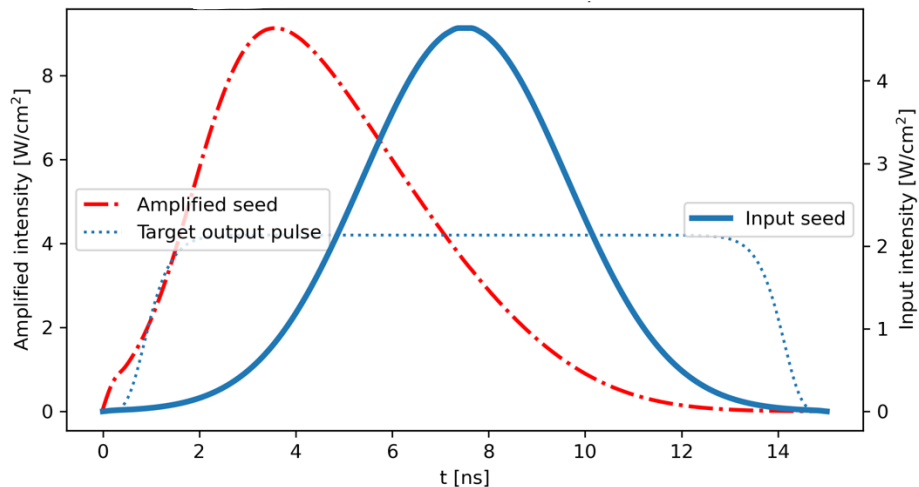
Phoenix – SBS cell



Proof-of-concept numerical experiment



Simulation - SBS in 1D (~40% amplification)



$$\left(\frac{\partial}{\partial t} - c\frac{\partial}{\partial z}\right) I_s = c\gamma_B g(\omega_a) I_s I_o$$

$$\left(\frac{\partial}{\partial t} + c\frac{\partial}{\partial z}\right) I_o = -c\gamma_B g(\omega_a) I_s I_o$$

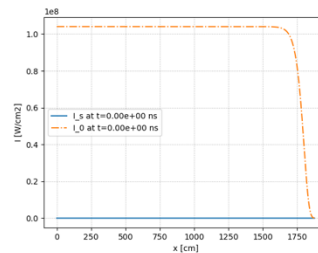
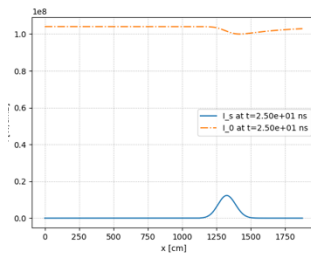
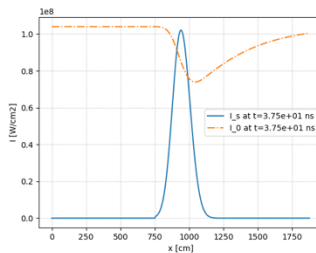
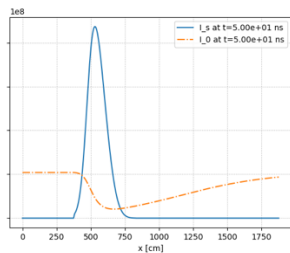
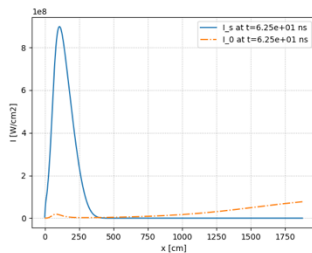
Integration after change of variables to coordinates co-moving with I_o and I_s

J. Murray et al., "Raman pulse compression of excimer lasers for application to laser fusion," IEEE Journal of Quantum Electronics, 15(5) 342 (1979).

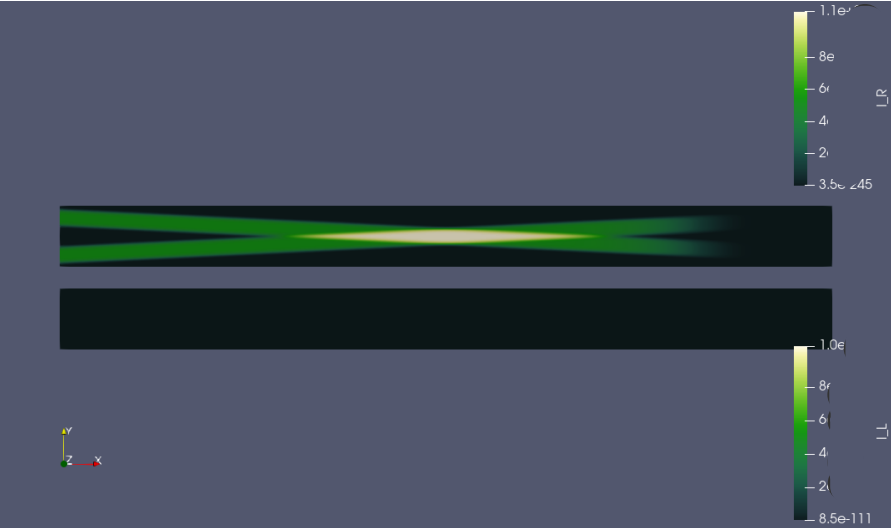
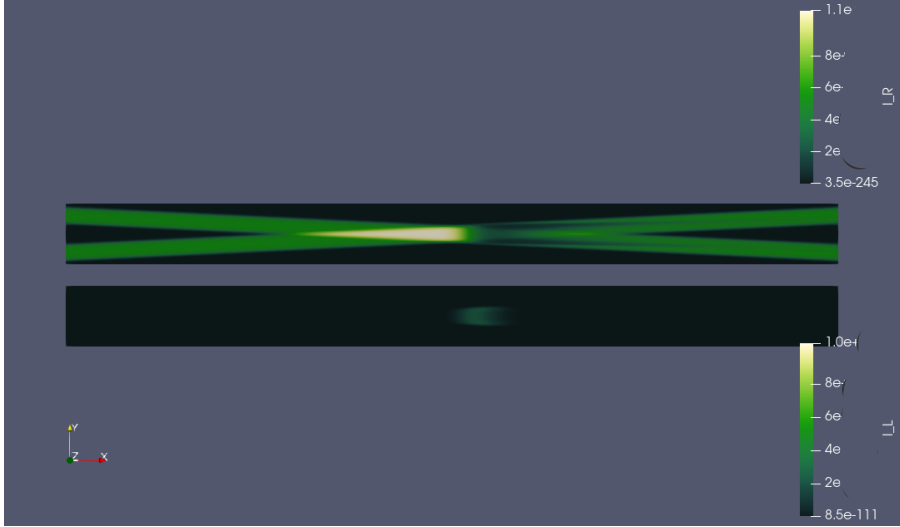
$$F_s^{out} / F_{sat} = \ln \left[1 + e^{F_o^{in} / F_{sat}} \left(e^{F_s^{in} / F_{sat}} - 1 \right) \right]$$

$$F_{sat} = \frac{2}{c\gamma_B} \quad L_{int} = \frac{\tau_p c}{2} \quad F_o^{in} = \int I_o(t_1, z) \frac{dz}{c}$$

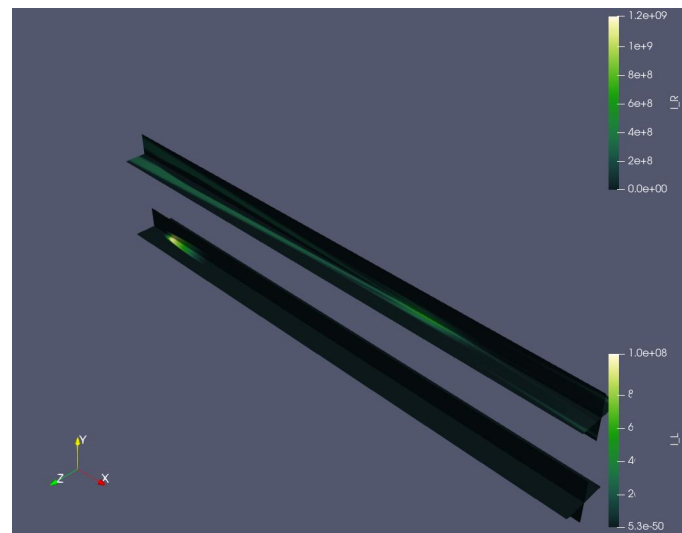
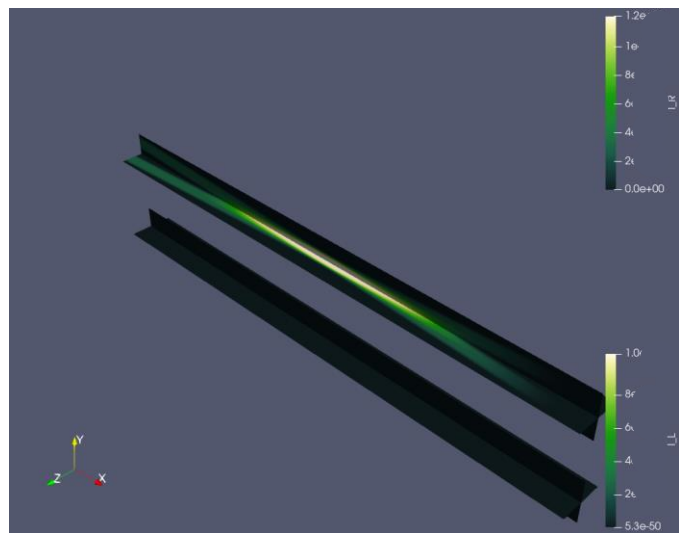
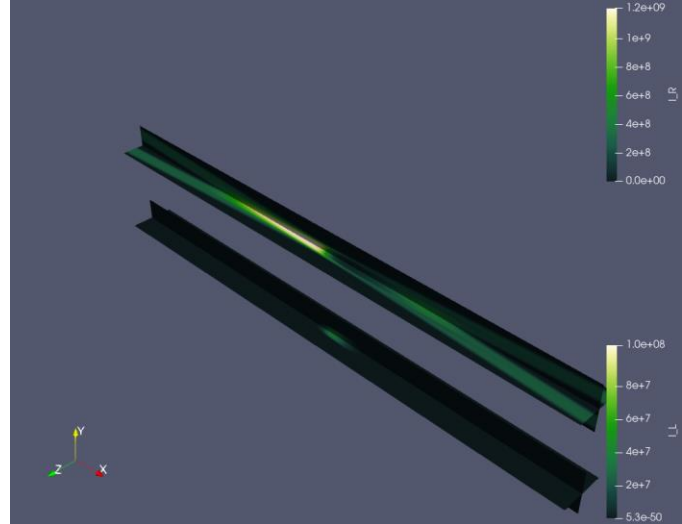
Fluence rerr $\sim 10^{-6}$ vs. analytic solution



Simulation - SBS in 2D



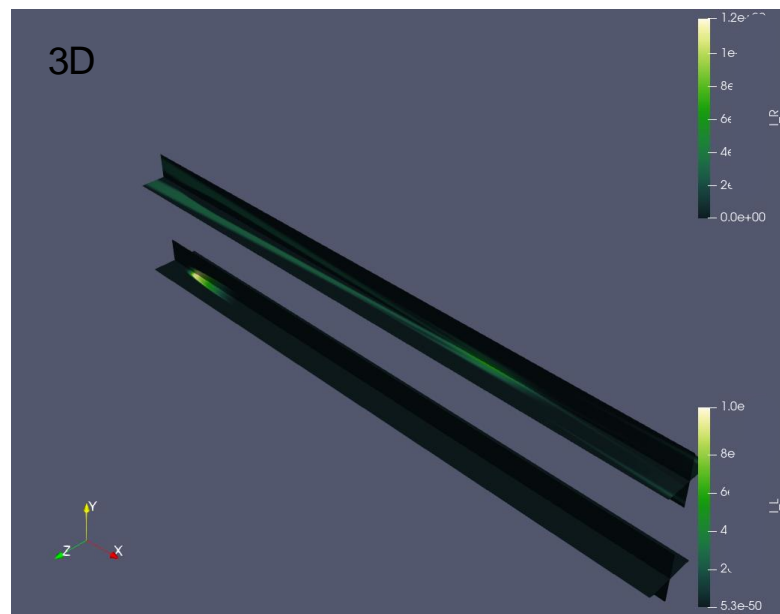
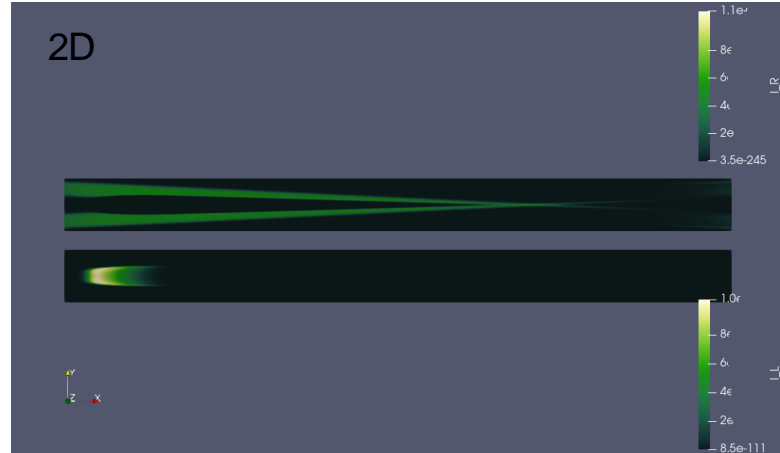
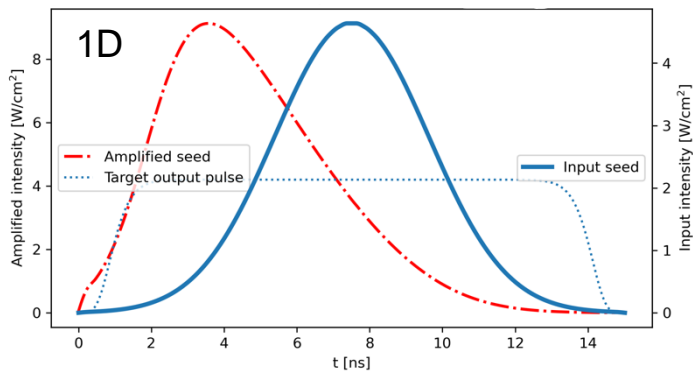
Simulation - SBS in 3D



Simulation – 1D/2D/3D physics validation

- Realistic Phoenix dimensions and geometry
- High-order Finite Element Method
- Based on MFEM open-source library
- Consistent seed amplification in 1D, 2D, and 3D
- 3D requires massively parallel simulations

Efficient design of Phoenix system
leveraging super-fast 1D, geometrically consistent 2D,
and complete 3D physics simulations!



Diffraction benchmark

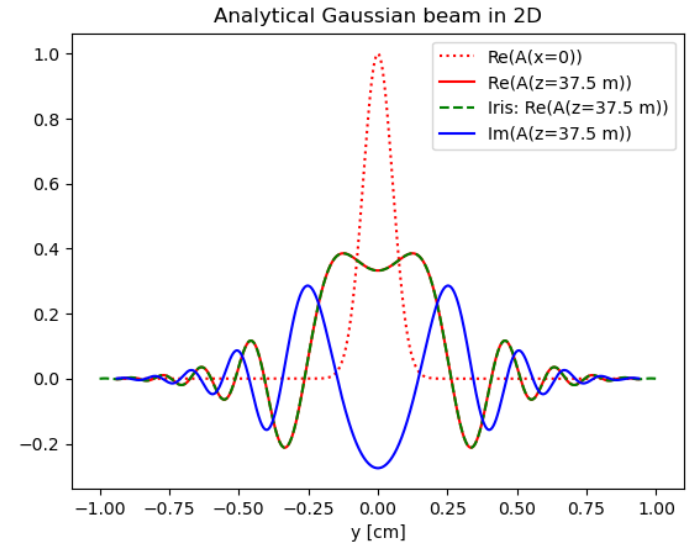
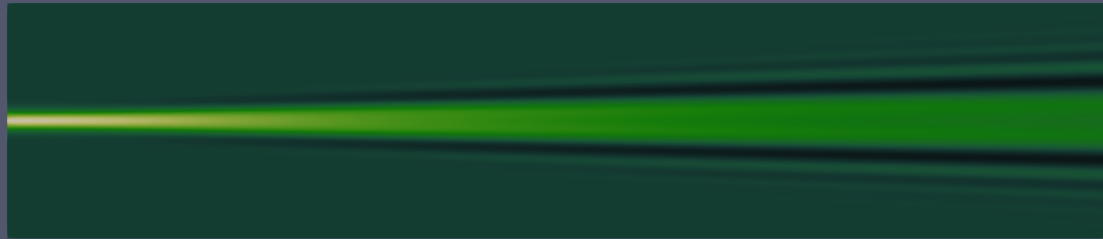
$$\partial_t A_0 + \frac{c \hat{\mathbf{k}}_0}{n} \cdot \nabla A_0 - \frac{ic}{2nk_0} \nabla^2 A_0 = -R |A_s|^2 A_0, \quad (10)$$

$$\partial_t A_s + \frac{c \hat{\mathbf{k}}_s}{n} \cdot \nabla A_s - \frac{ic}{2nk_s} \nabla^2 A_s = R^* |A_0|^2 A_s, \quad (11)$$

Benchmark: Gaussian beam in 2D and 3D
rerr 10⁻³ vs analytical solution
4th order accurate scheme



Only 3 elements over the Gaussian feature
16x more accurate for dx/2

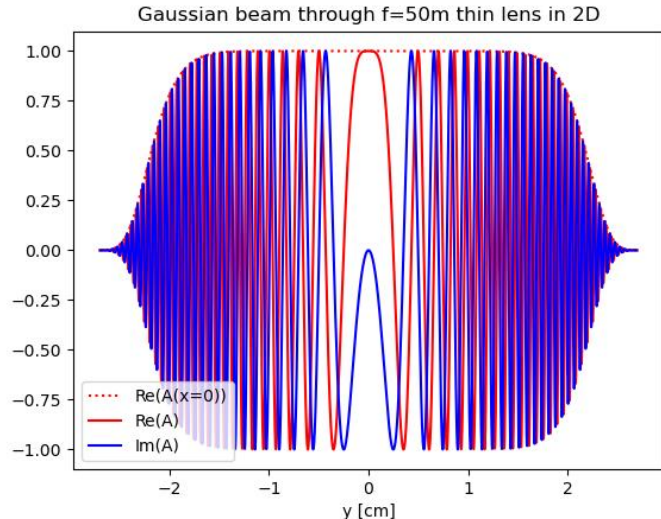


Phase transformations

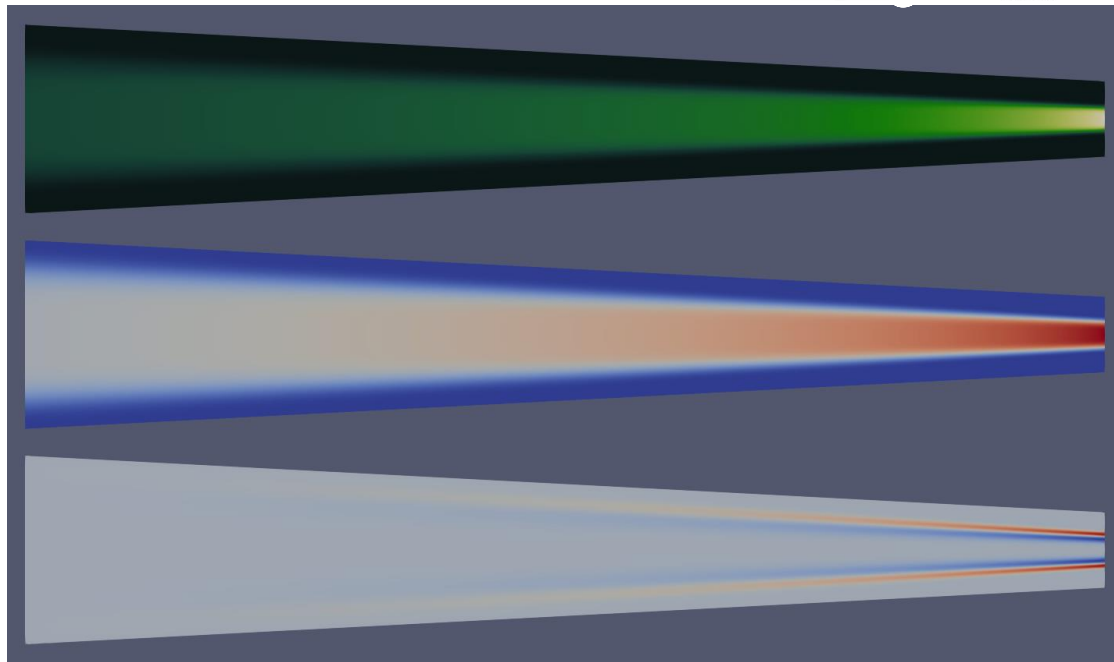
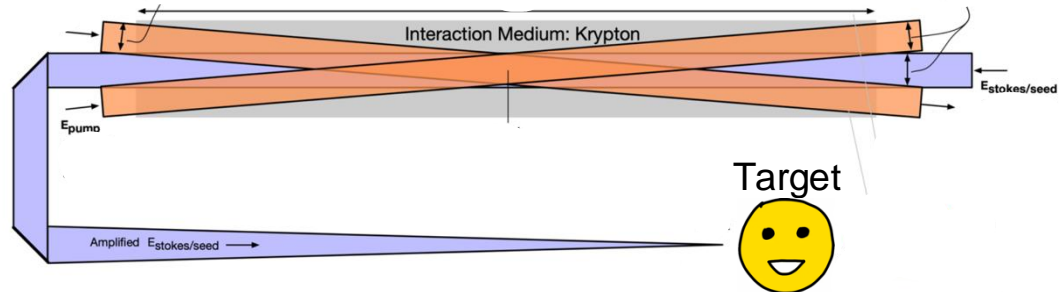
lens/phase-plate

Focusing element

- proof-of-concept of target irradiation
- improved accuracy by wedged mesh
- Serious high-frequency pollution!

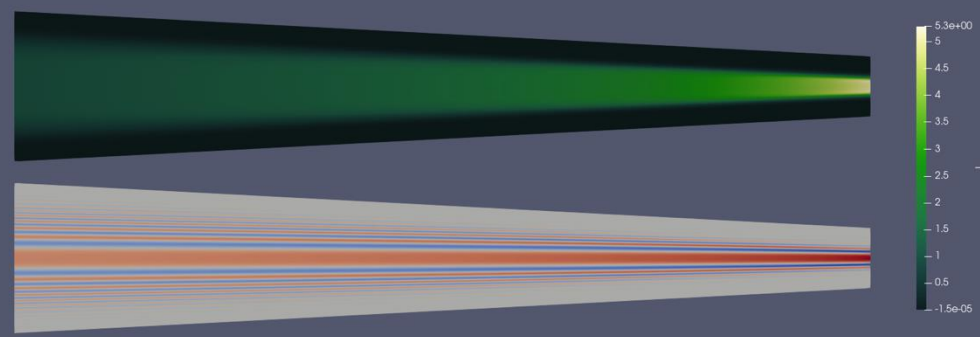


$$u_g(x, y, z, t) = a_0(x, y, z, t) \exp \left(i \left(|\vec{k}| (z + f(x, y, z)) - \omega t \right) \right)$$

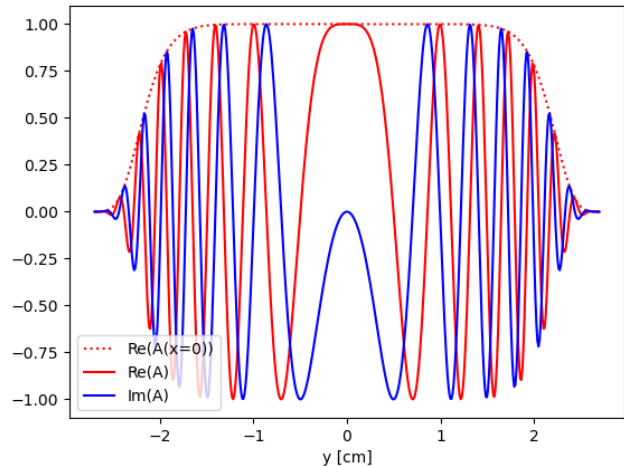


Phase transformation 200m lens/phase-plate

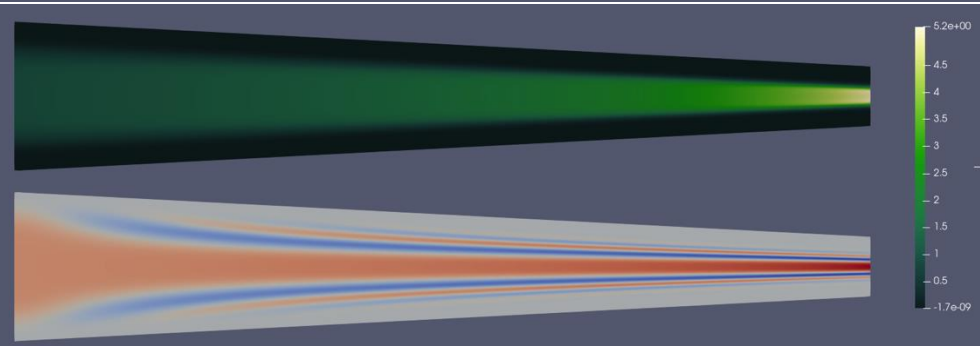
plane phase



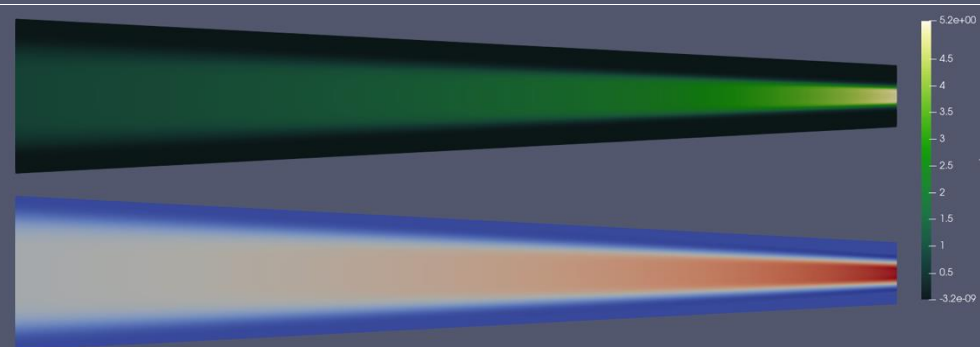
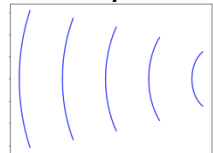
Gaussian beam through $f=200\text{m}$ thin lens in 2D



incoming phase



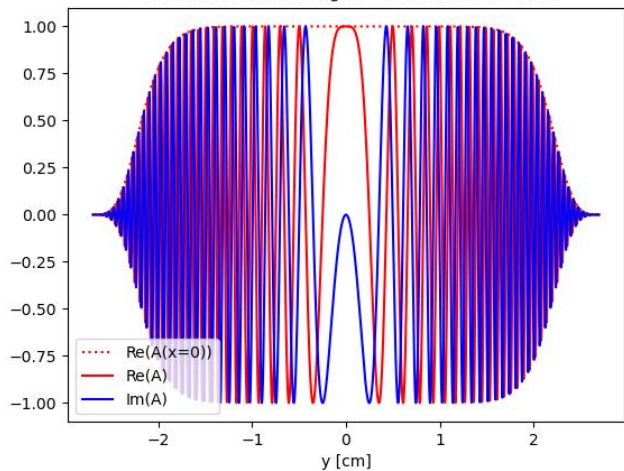
exact phase



wavelength $2.1e-01$ [cm] requires $6.2e+02$ DOFs ($p=3$)

Phase transformation 50m lens/phase-plate

Gaussian beam through $f=50\text{m}$ thin lens in 2D



wavelength $5.4\text{e-}02$ [cm] requires $2.4\text{e+}03$ DOFs ($p=3$)

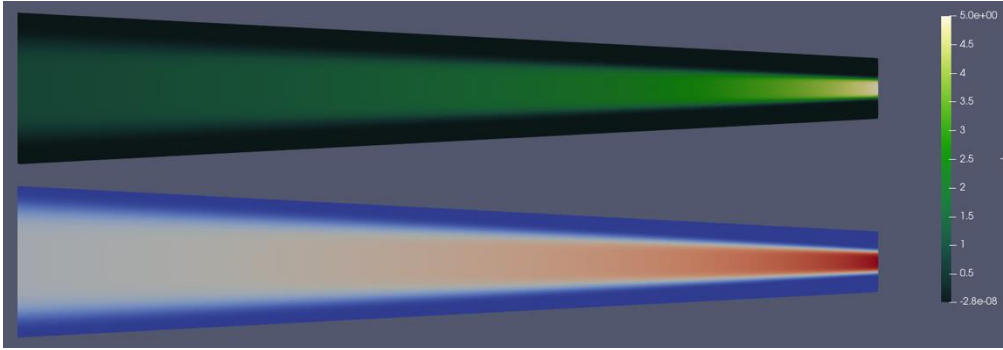
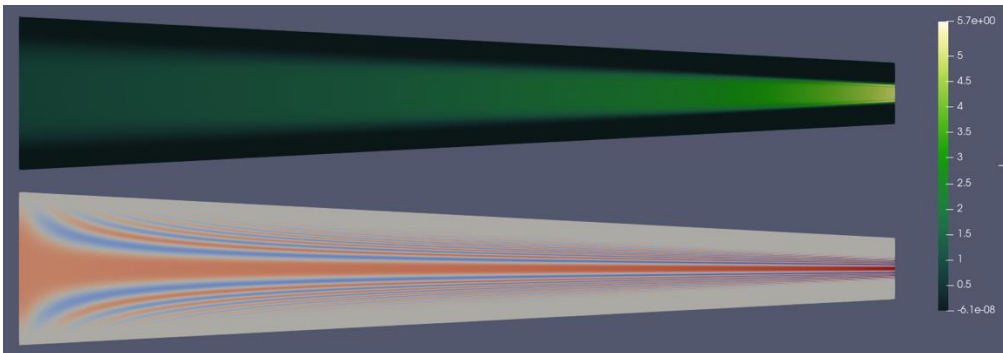
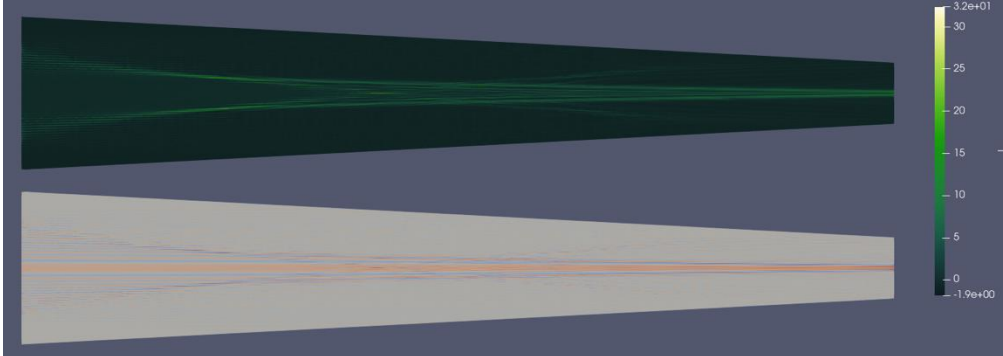
XEC

plane phase



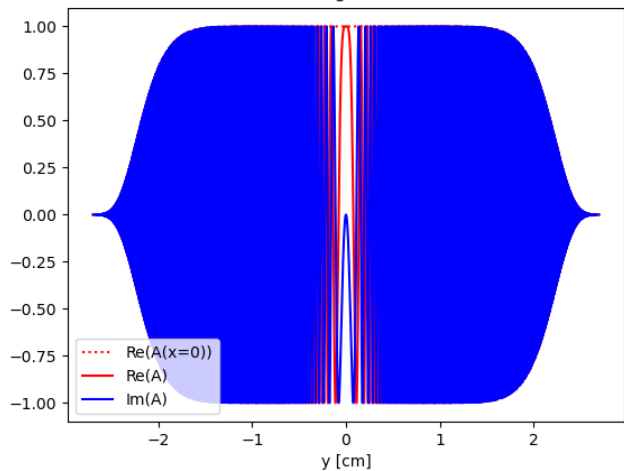
incoming phase

exact phase



Phase transformation 5m lens/phase-plate

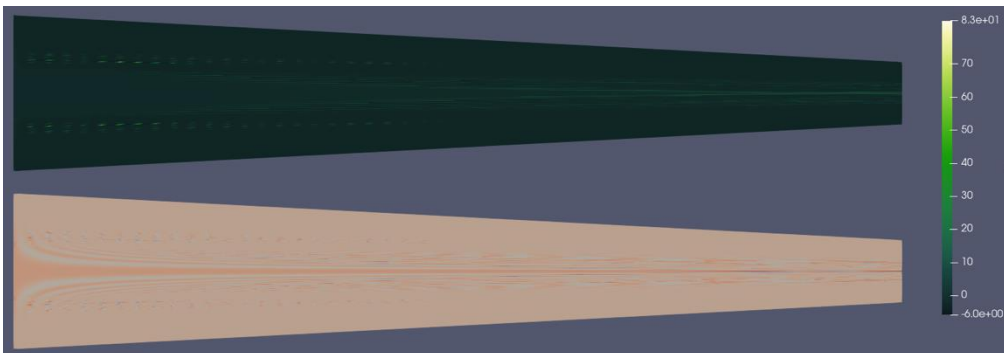
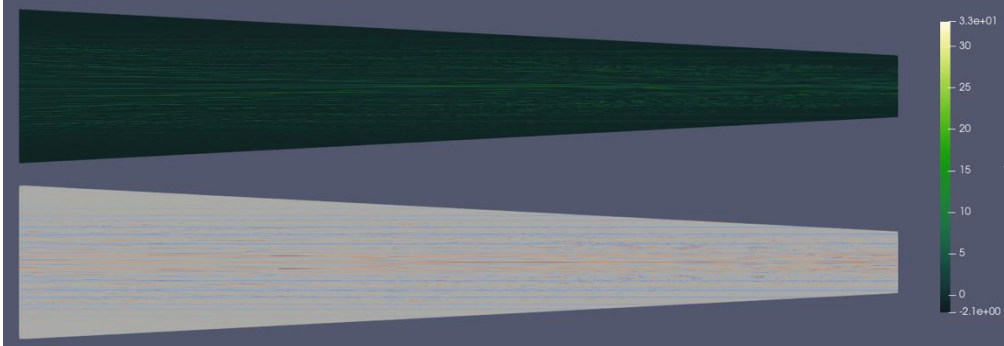
Gaussian beam through $f=5\text{m}$ thin lens in 2D



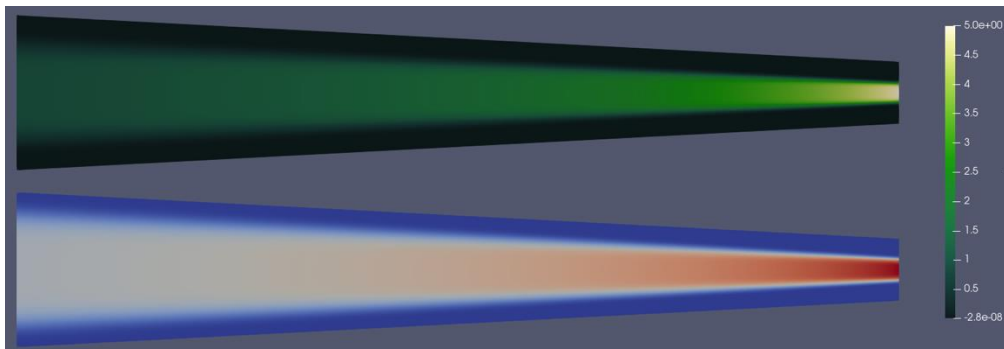
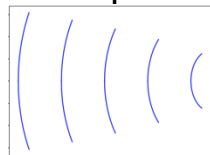
plane phase



incoming phase



exact phase



wavelength $5.5e-03$ [cm] requires $2.4e+04$ DOFs ($p=3$)

Smart transform $\sim 1e6$ x less DOFs!

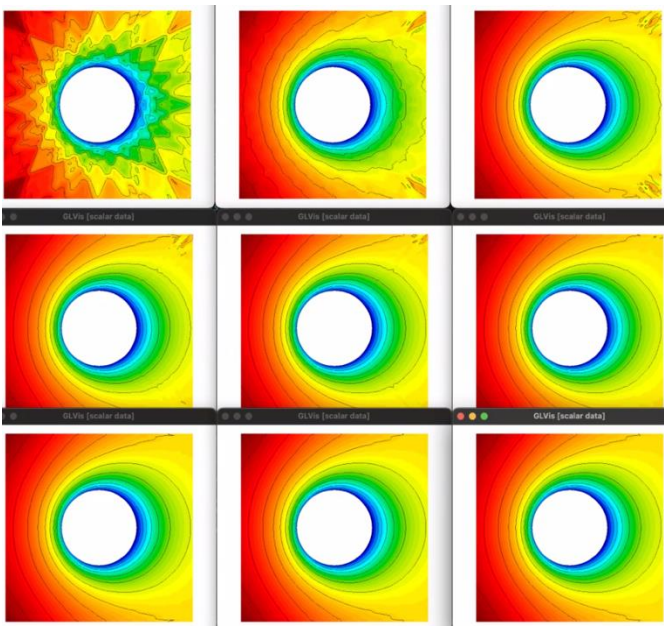
XEC



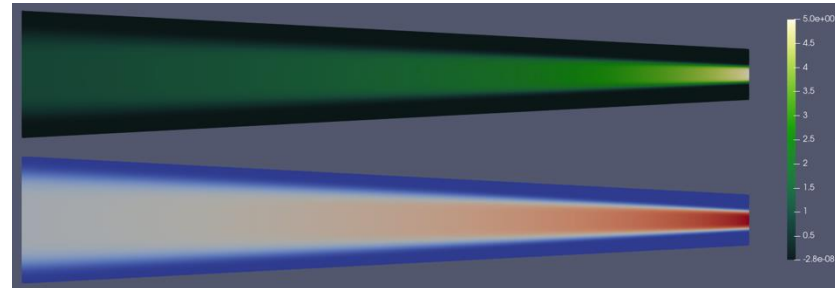
Takeaway: MFEM + smart coordinate transforms rock!

- Complex high-order DG (p=3), no-upwind, symplectic time

Accurate & robust Boltzmann physics
General-S_N the fastest HPC framework



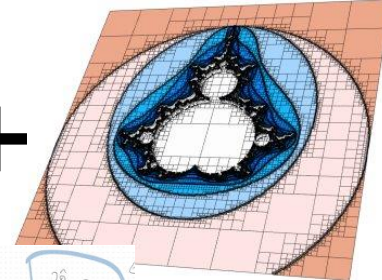
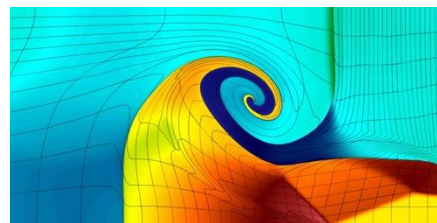
$$u_g(x, y, z, t) = a_0(x, y, z, t) \exp(i(|\vec{k}|(z + f(x, y, z)) - \omega t))$$



Efficient IFE design (user friendly direct ALE)

Lagrangian hydro

Eulerian hydro



$$\begin{aligned} \frac{\partial \xi}{\partial t} + \nabla \cdot [\xi (\mathbf{u}^* - \mathbf{u}) \cdot \mathbf{e}_i] &= 0 \\ \frac{\partial \xi \mathbf{u}}{\partial t} + \nabla \cdot [\xi \mathbf{u} \otimes (\mathbf{u}^* - \mathbf{u}) + \mathbf{p} \mathbf{I}] \cdot \mathbf{e}_i &= 0 \\ \frac{\partial \xi}{\partial t} + \nabla \cdot [\xi (\mathbf{u}^* - \mathbf{u}) + \mathbf{p} \mathbf{e}_i] \cdot \mathbf{e}_i &= 0 \\ \frac{d\xi}{dt} = \mathbf{u}^* \cdot \nabla \xi &= 0 \end{aligned} \quad \Rightarrow \quad \begin{aligned} \frac{\partial \xi}{\partial t} &= 0 \\ \frac{\partial \xi \mathbf{u}}{\partial t} &= -\frac{1}{\xi} \nabla \cdot \mathbf{p} \\ \xi \frac{\partial \xi}{\partial t} &= -\mathbf{p} \cdot \nabla \xi \end{aligned}$$